École Doctorale des Sciences de l'Environnement d’Île-de-France

Année Universitaire 2014-2015

Modélisation Numérique de l’Écoulement Atmosphérique et Assimilation de Données

Olivier Talagrand
Cours 2

2 Avril 2015

Lois physiques doivent en pratique être discrétisées dans le temps et dans l'espace ⇒ *modèles numériques*, nécessairement imparfaits.

Les modèles utilisés pour la prévision météorologique de grande échelle et la simulation climatologique couvrent la totalité du volume de l'atmosphère. Ils sont, jusqu'à présent au moins, construits sur l'hypothèse *hydrostatique*

Dans la direction verticale :

$$\partial p/\partial z + \rho g = 0$$

Élimine l'équation du mouvement pour la direction verticale; en outre, l'écoulement est incompressible dans les coordonnées (x, y, p) ⇒ nombre d'équations diminué de deux unités.

Approximation hydrostatique valide pour échelles horizontales > 20-30 km

Modèles non-hydrostatiques, plus coûteux, sont utilisés pour la météorologie de petite échelle.

Modèles (semi-)spectraux

$$T(\mu=\sin(\text{latitude}),\ \lambda=\text{longitude}) = \sum_{\substack{0\le n<\infty \\ -n\le m\le n}} T_n^m Y_n^m(\mu,\lambda)$$

où les $Y_n^m(\mu,\lambda)$ sont les *harmoniques sphériques*

$$Y_n^m(\mu,\lambda) \propto P_n^m(\mu)\exp(im\lambda)$$

$P_n^m(\mu)$ est la *fonction de Legendre* de deuxième espèce.

$$P_n^m(\mu) \propto (1-\mu^2)^{\frac{m}{2}} \frac{d^{n+m}}{d\mu^{n+m}}(\mu^2-1)^n$$

n et m sont respectivement le *degré* et l'*ordre* de l’harmonique $Y_n^m(\mu,\lambda)$

From Wikipedia, the free encyclopedia

$l = 3$
$m = 0$
$l\text{-}m = 3$

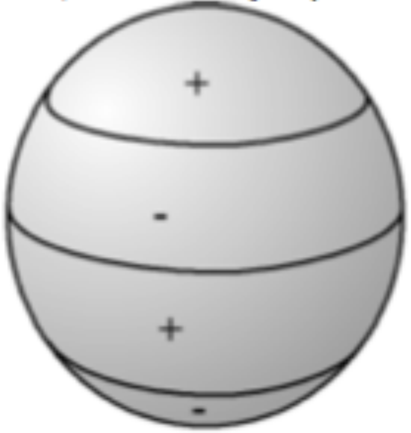

$l = 3$
$m = 1$
$l\text{-}m = 2$

$l = 3$
$m = 2$
$l\text{-}m = 1$

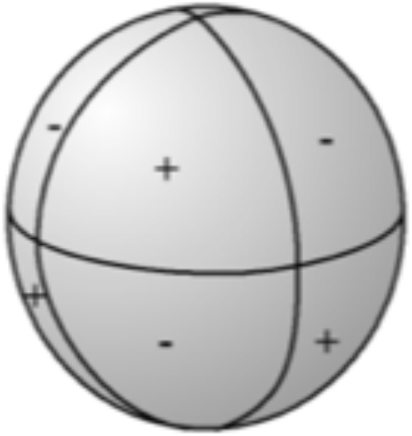

$l = 3$
$m = 3$
$l\text{-}m = 0$

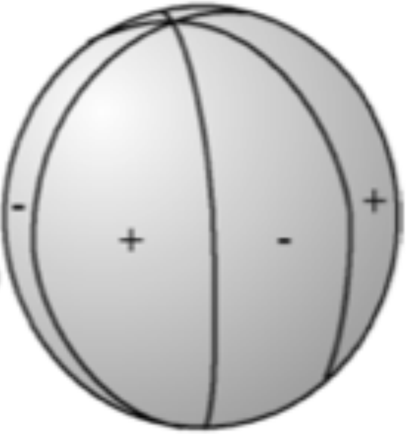

$l = 5$
$m = 2$
$l\text{-}m = 3$

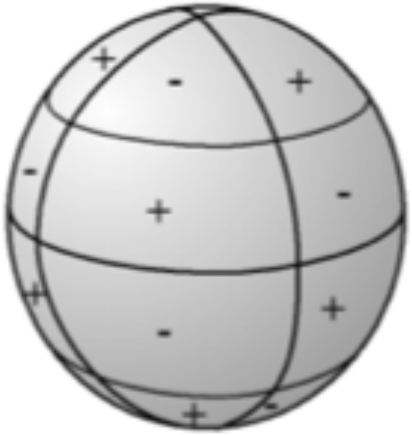

Modèles (semi-)spectraux

Les harmoniques sphériques définissent une base complète orthonormée de l'espace L^2 à la surface S de la sphère.

$$\int_S Y_n^m Y_{n'}^{m'} \, d\mu d\lambda = \delta_n^{n'} \delta_m^{m'}$$

Relation de Parseval

$$\int_S T^2(\mu,\lambda) \, d\mu d\lambda = \sum_{\substack{0 \le n < \infty \\ -n \le m \le n}} \left| T_n^m \right|^2$$

Les harmoniques sphériques sont fonctions propres du laplacien à la surface de la sphère

$$\Delta Y_n^m = -n(n+1)Y_n^m$$

Troncature ‘triangulaire’ *TN* ($n \leq N$, $-n \leq m \leq n$) indépendante du choix d’un axe polaire. Représentation est parfaitement homogène à la surface de la sphère

Calculs non linéaires effectués dans l’espace physique (sur grille latitude-longitude ‘gaussienne’). Les transformations requises sont possibles à un coût non prohibitif grâce à l’utilisation de Transformées de Fourier Rapides (*Fast Fourier Transforms*, *FFT*, en anglais). Il existe aussi une version rapide des Transformées de Legendre, relatives à la variable μ.

Pressure p, although convenient for writing down the equations, is in fact rather inconvenient because lower boundary is not fixed in (x, y, p)-space.

So-called σ-coordinate. $\sigma \equiv p/p_S$, where p_S is pressure at ground level.

‘Hybrid’ coordinate.

Temporal discretization. Courant-Friedrichs-Lewy (CFL) condition for stability of explicit schemes

$$\Delta t / \Delta x < \alpha / c$$

where c is phase velocity of fastest propagating (wave) in the system, and α is an $O(1)$ numerical coefficient depending on particular scheme under consideration.

Significance : numerical propagation of signal must be at least as fast as physical propagation.

In hydrostatic atmosphere, fastest propagating wave : gravity wave with largest scale height, $c = \sqrt{(rT)} \approx 300$ m.s^{-1}.

$$\Delta x = 30 \text{ km} \qquad \Rightarrow \quad \Delta t = 100 \text{ s}$$

The use of *semi-implicit* schemes allows to get rid of the CFL condition, and to use longer timesteps.

In the parlance of the trade, one distinguishes two different parts in models. The 'dynamics' deals with the physically reversible processes (pressure forces, Coriolis force, advection, ...), while the 'physics' deals with physically irreversible processes, in particular the diabatic heating term Q in the energy equation, and also the parameterization of subgrid scales effects.

Numerical schemes have been progressively developed and validated for the 'dynamics' component of models, which are by and large considered now to work satisfactorily (although regular improvements are still being made; project *DYNAMICO*, *Dynamical Core on Icosahedral Grid*, Th. Dubos, IPSL).

The situation is different as concerns ‘physics’, where many problems remain (as concerns for instance subgrid scales parameterization, the water cycle and the associated exchanges of energy, or the exchanges between the atmosphere and the underlying medium). ‘Physics’ as a whole remains the weaker point of models, and is still the object of active research.

5 - SCHEMA DES INTERACTIONS PHYSIQUES DANS LE MODELE

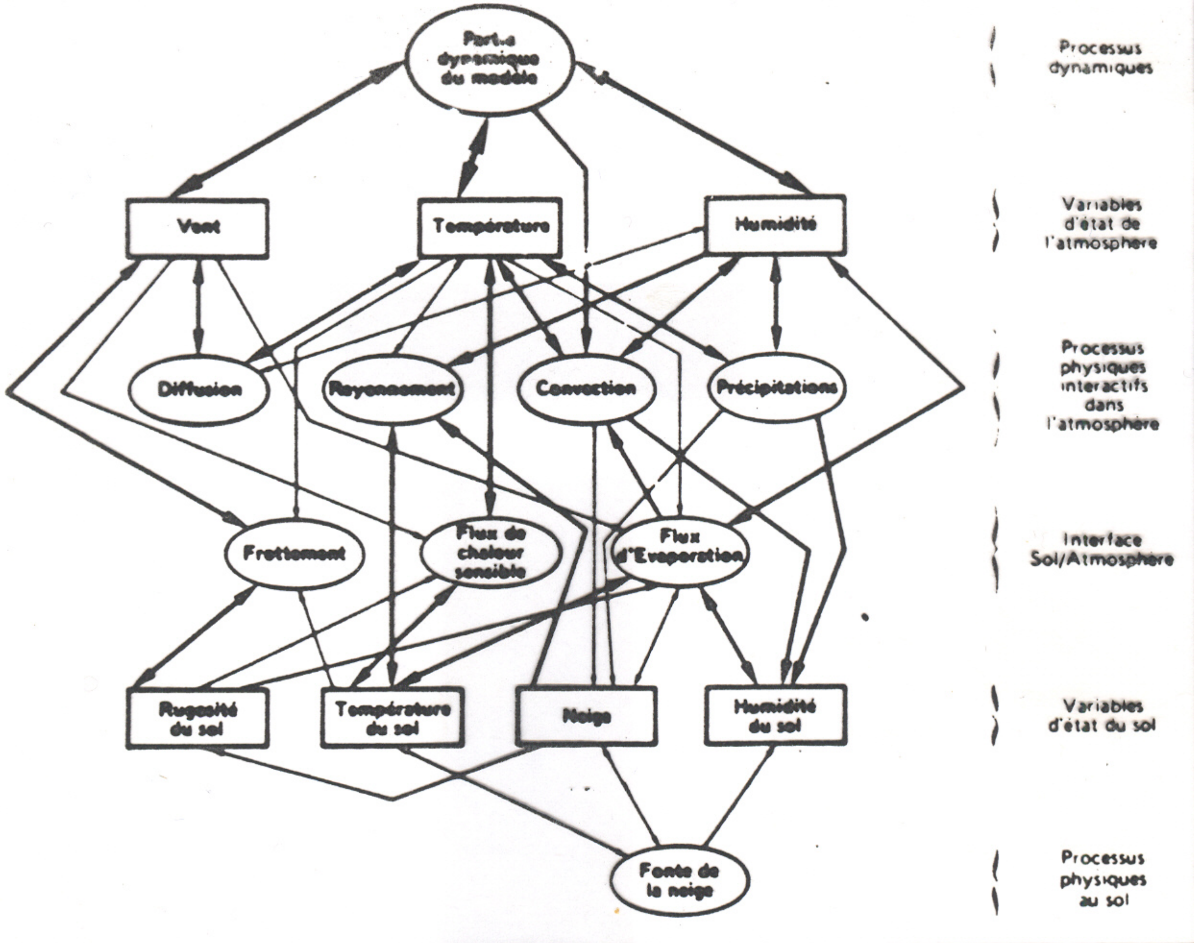

Centre Européen pour les Prévisions Météorologiques à Moyen Terme (CEPMMT, Reading, GB)

(European Centre for Medium-range Weather Forecasts, ECMWF)

Depuis juin 2013 :

Troncature triangulaire T1279 (résolution horizontale ≈ 16 kilomètres)

137 niveaux dans la direction verticale (0 - 80 km)

Dimension du vecteur d'état correspondant ≈ $2{,}3\ 10^9$

Pas de discrétisation temporelle (schéma semi-Lagrangien semi-implicite): 10 minutes

Wednesday 25 March 2015 12UTC ©ECMWF Forecast t+144 VT: Tuesday 31 March 2015 12UTC
Surface: Mean sea level pressure / 850-hPa wind speed

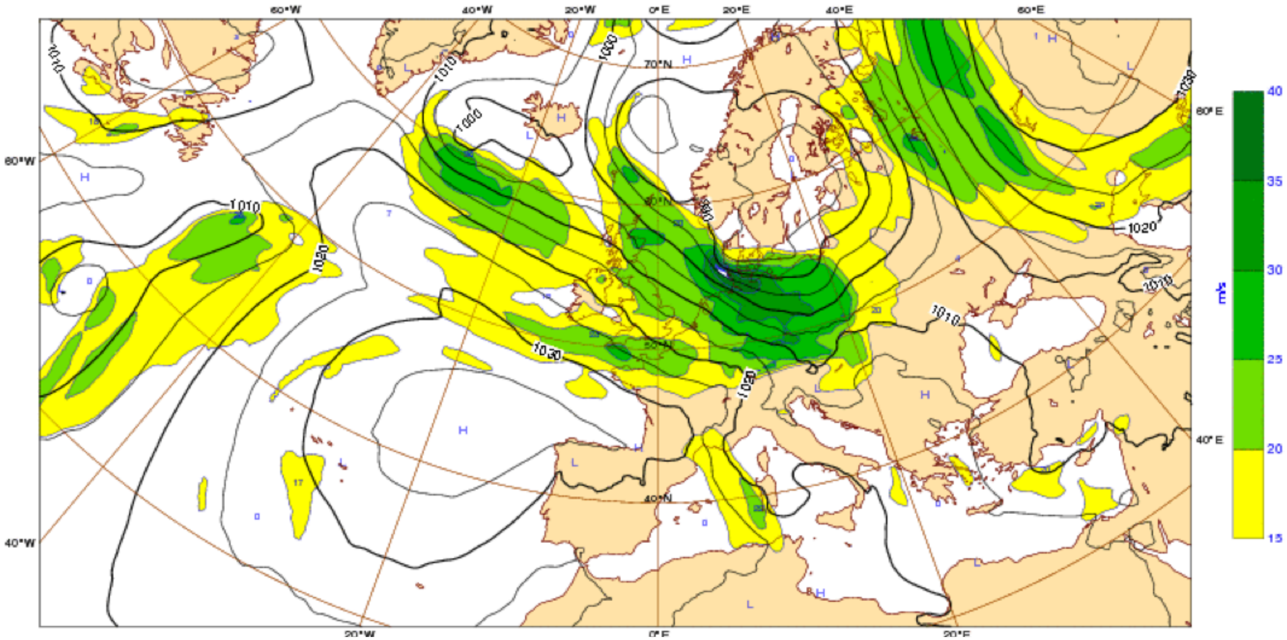

Tuesday 31 March 2015 12UTC ©ECMWF Analysis t+000 VT: Tuesday 31 March 2015 12UTC
Surface: Mean sea level pressure / 850-hPa wind speed

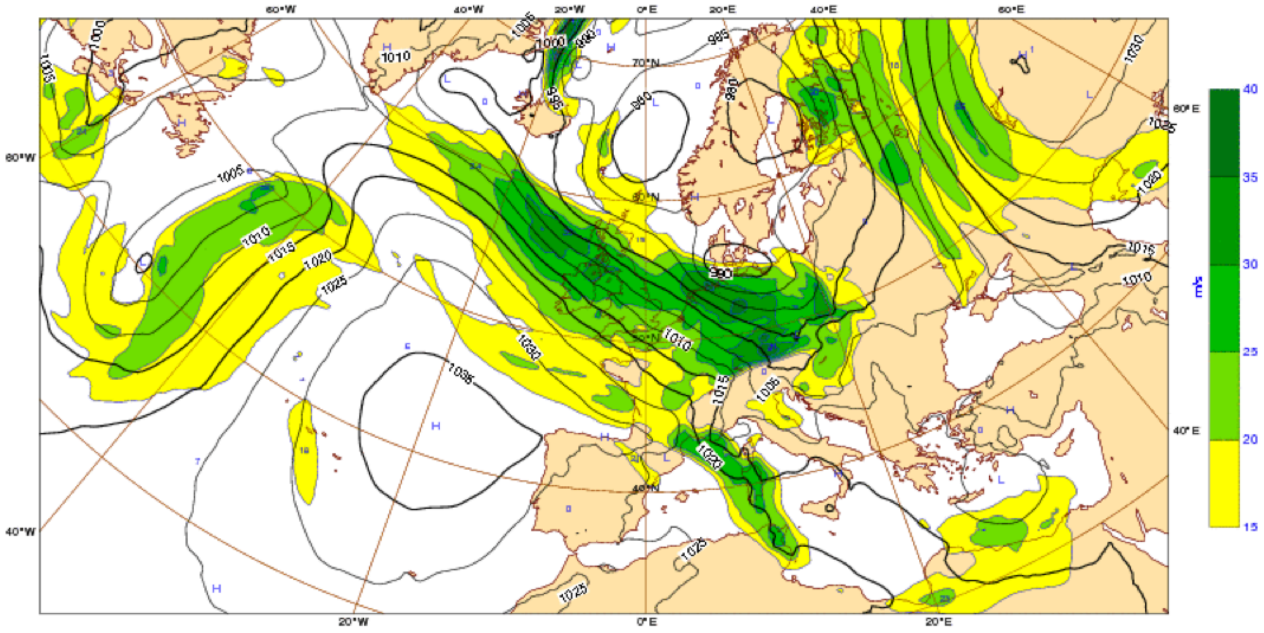

Wednesday 25 March 2015 12UTC ©ECMWF Analysis t+000 VT: Wednesday 25 March 2015 12UTC
Surface: Mean sea level pressure / 850-hPa wind speed

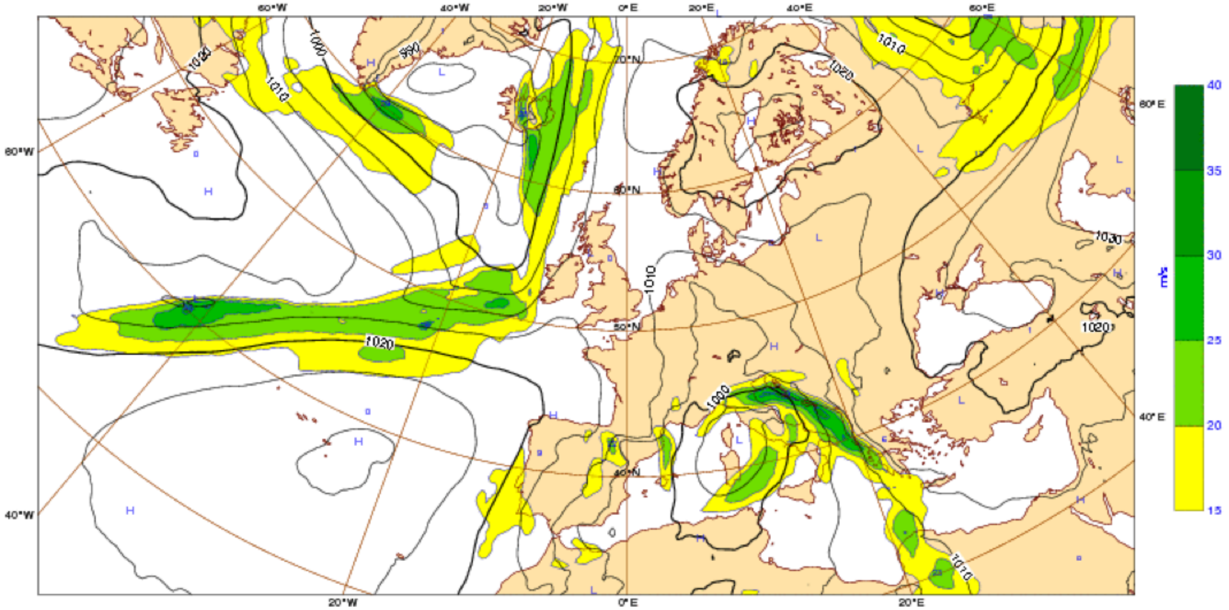

Tuesday 31 March 2015 12UTC ©ECMWF Analysis t+000 VT: Tuesday 31 March 2015 12UTC
Surface: Mean sea level pressure / 850-hPa wind speed

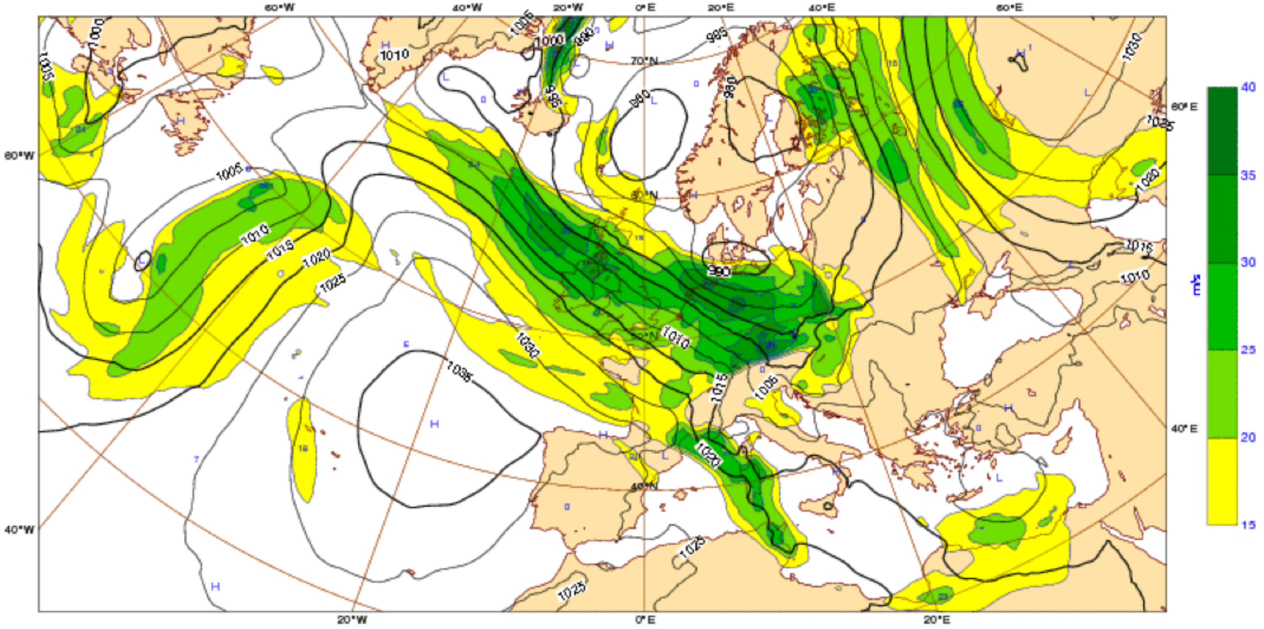

Résultats extraits de :

Haiden *et al.*, 2014, *Evaluations of ECMWF forecasts including 2013-2014 upgrades*, Memorandum Technique 742, CEPMMT, Reading, GB.

Disponible à l'adresse

http://old.ecmwf.int/publications/library/ecpublications/_pdf/tm/701-800/tm742.pdf

(voir aussi l'ensemble du site du CEPMMT)

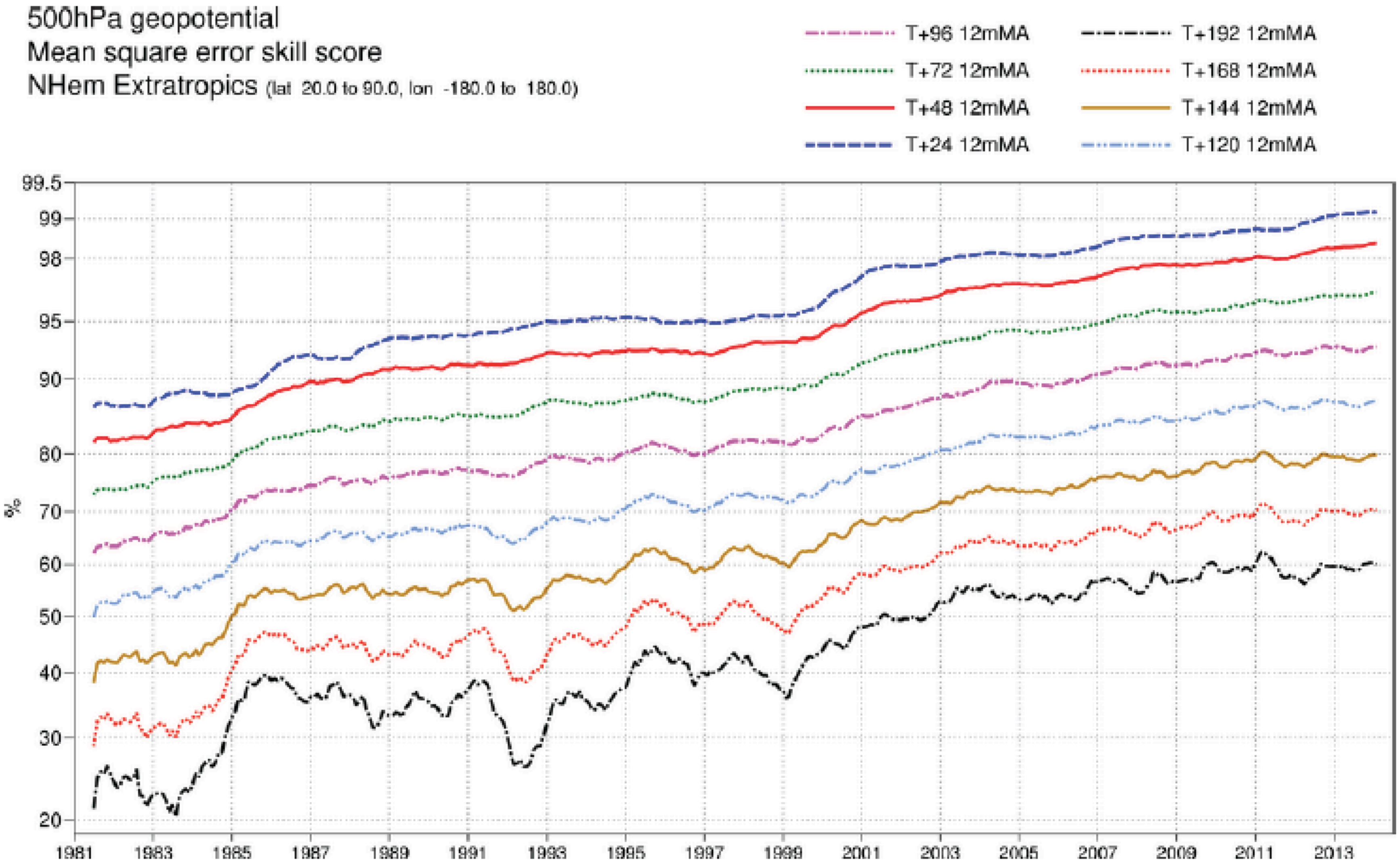

Figure 3: 500 hPa geopotential height mean square error skill score for Europe (top) and the northern hemisphere extratropics (bottom), showing 12-month moving averages for forecast ranges from 24 to 192 hours. The last point on each curve is for the 12-month period August 2013–July 2014.

Persistence = 0 ; climatology = 50 at long range

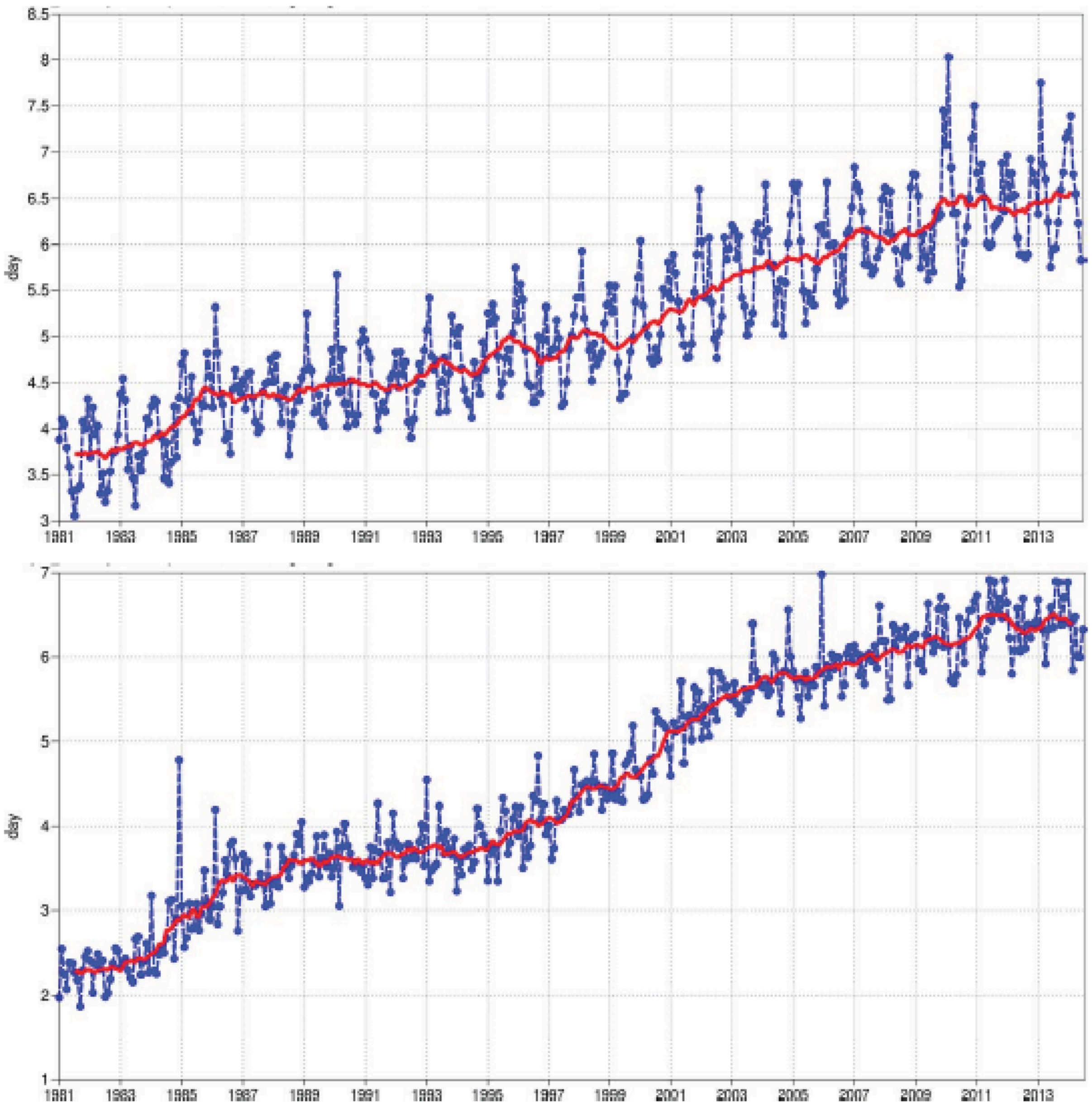

Figure 2: Primary headline score for the high-resolution forecasts. Evolution with time of the 500 hPa geopotential height forecast performance – each point on the curves is the forecast range at which the monthly mean (blue lines) or 12-month mean centred on that month (red line) of the forecast anomaly correlation (ACC) with the verifying analysis falls below 80% for Europe (top), northern hemisphere extratropics (centre) and southern hemisphere extratropics (bottom).

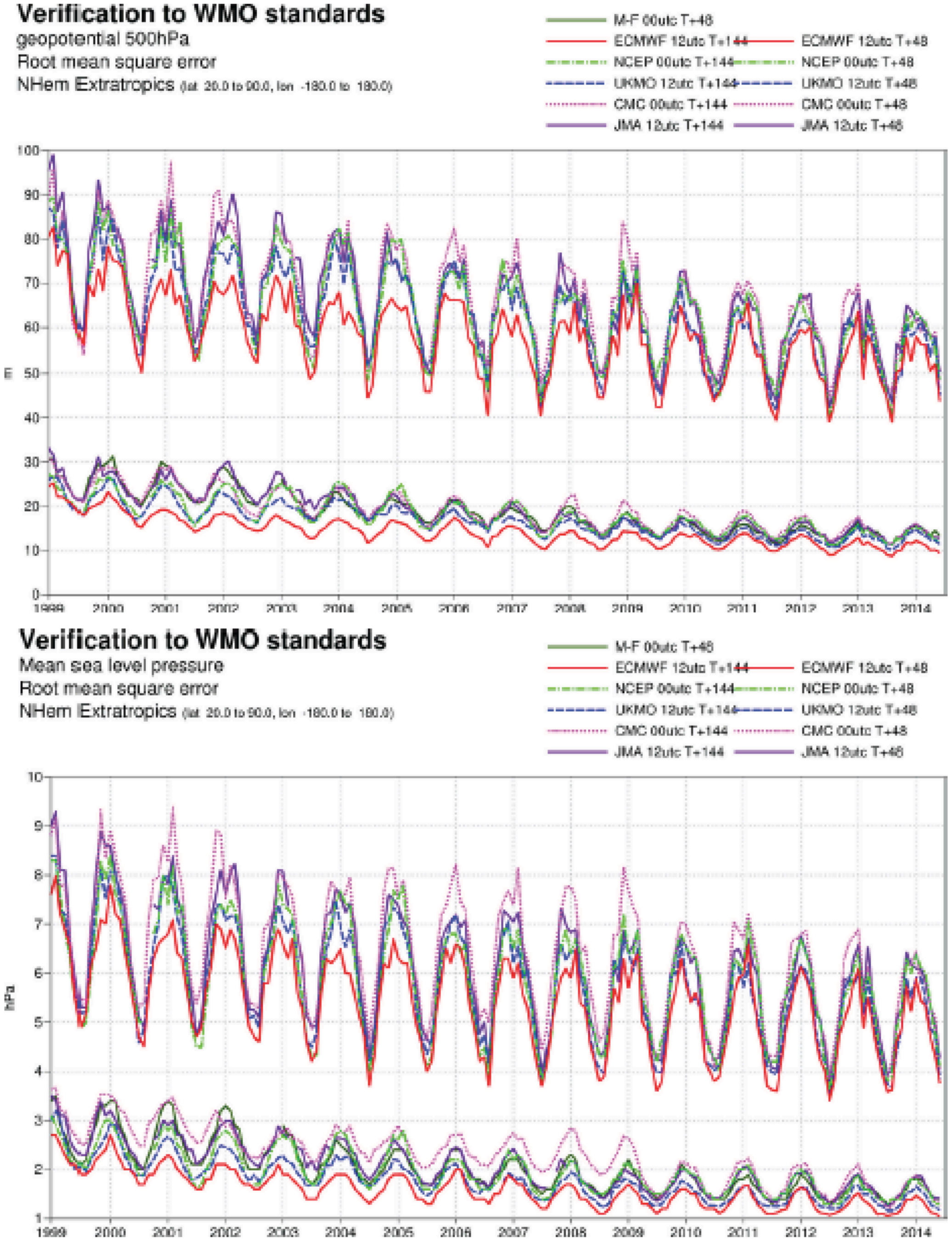

Figure 15: WMO-exchanged scores from global forecast centres. RMS error over northern extratropics for 500 hPa geopotential height (top) and mean sea level pressure (bottom). In each panel the upper curves show the

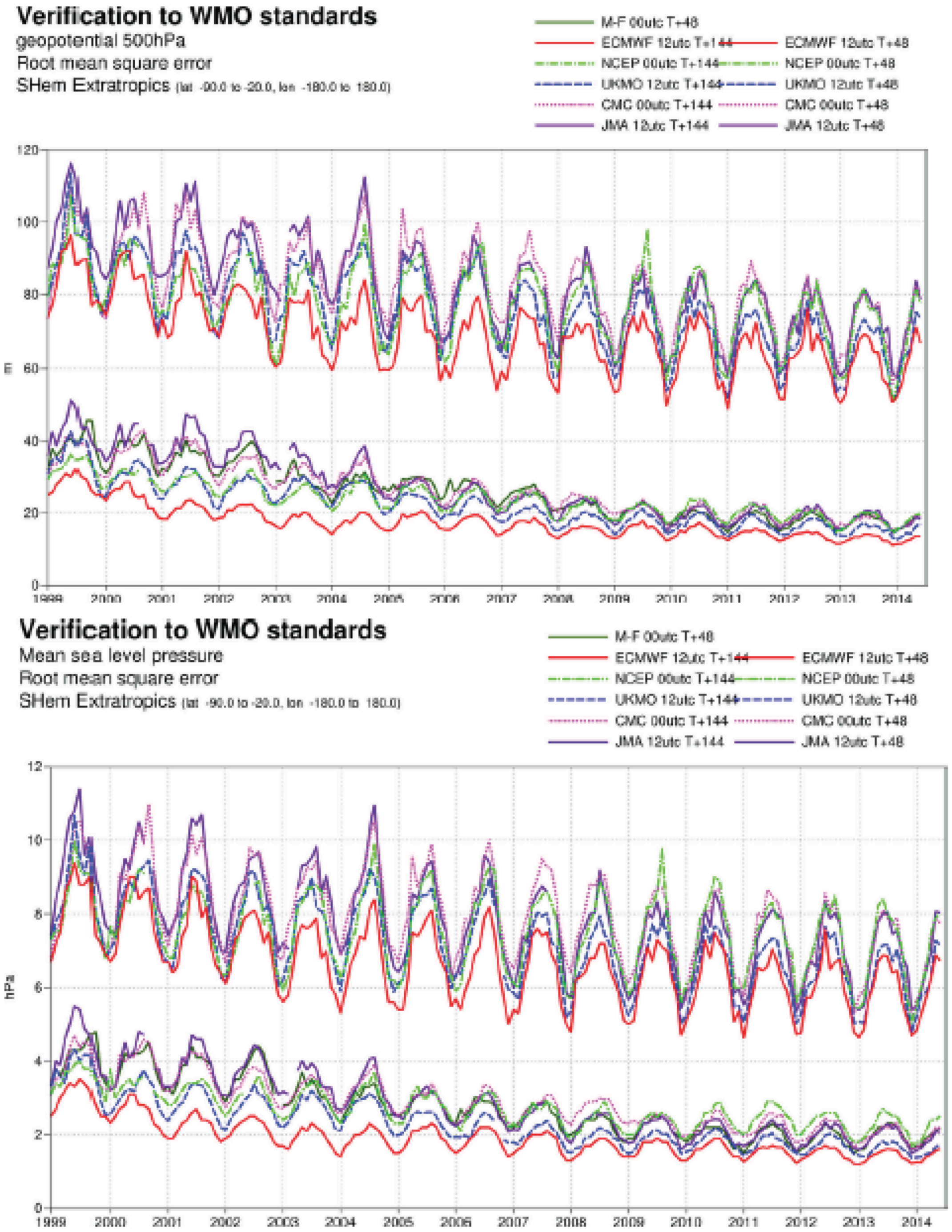

Figure 16: As Figure 15 for the southern hemisphere.

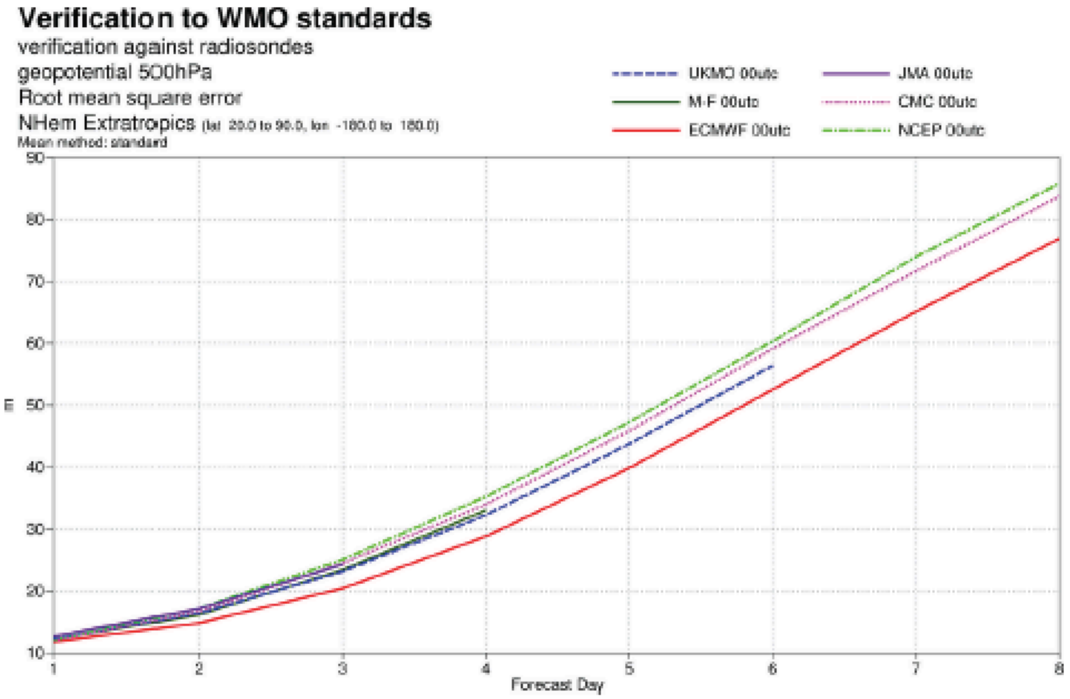

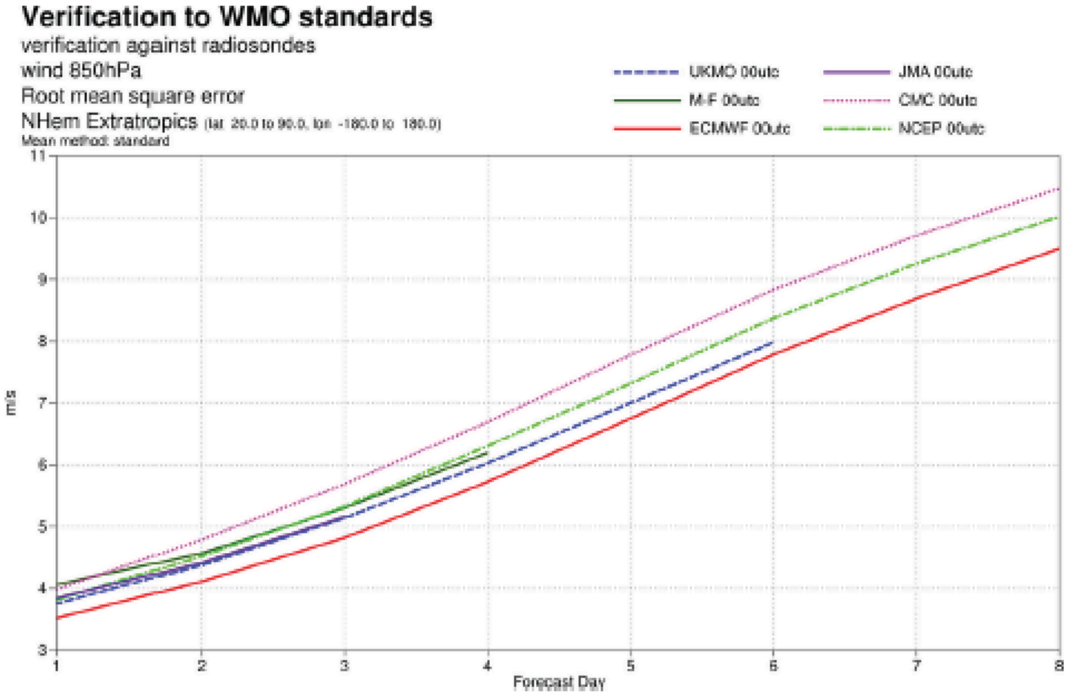

Annual mean
August 2013
– July 2014

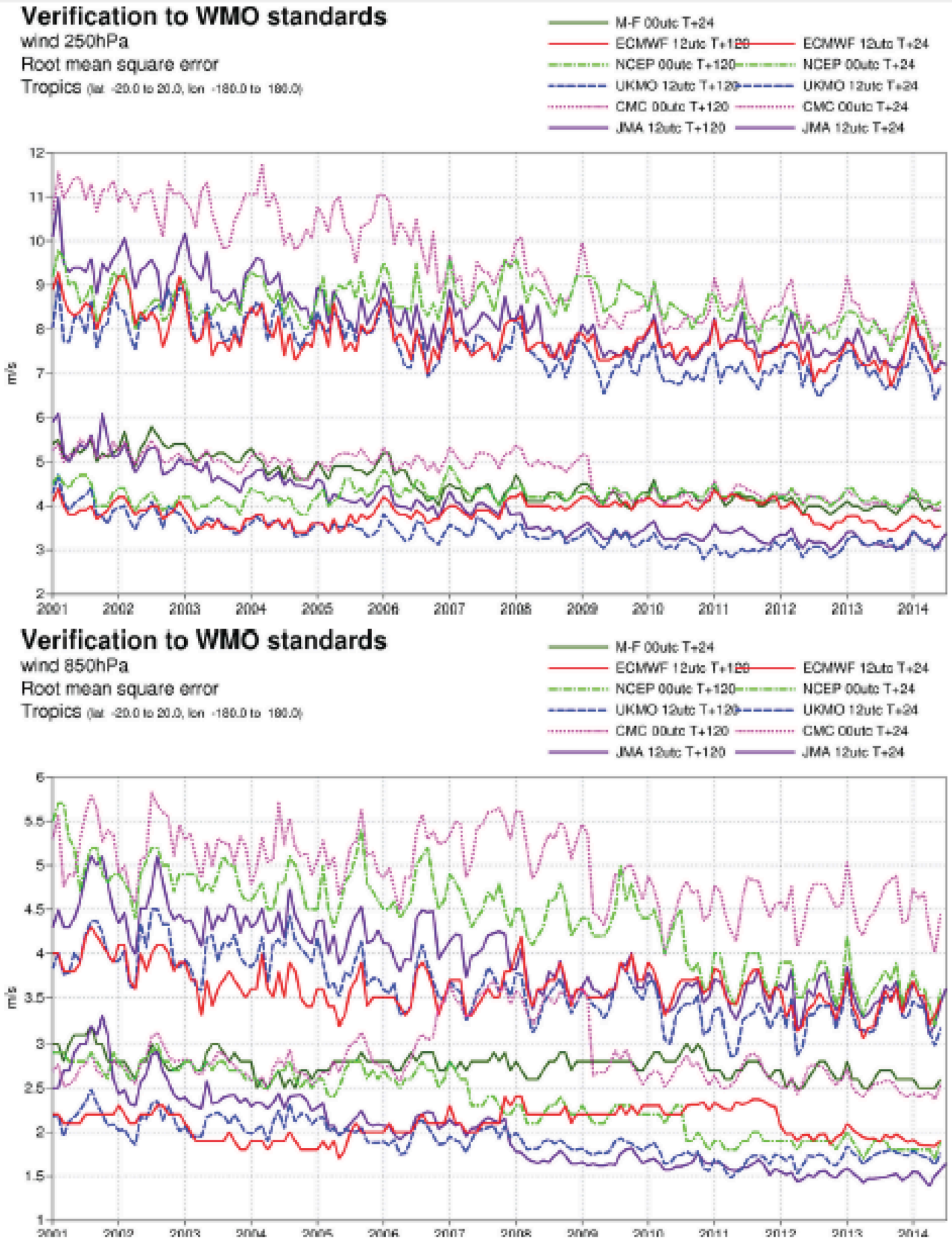

Figure 19: WMO-exchanged scores from global forecast centres. RMS vector wind error over tropics at 250 hPa (top) and 850 hPa (bottom). In each panel the upper curves show the five-day forecast error and the lower curves show the one-day forecast error. Each model is verified against its own analysis.

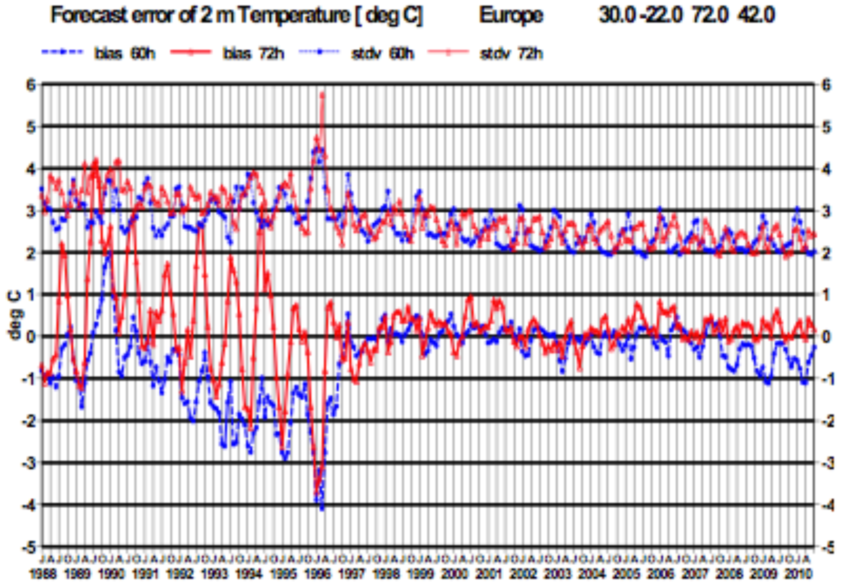

Figure 16: Verification of 2 metre temperature forecasts against European SYNOP data on the GTS for 60-hour (night-time) and 72-hour (daytime) forecasts. Lower pair of curves show bias, upper curves are standard deviation of error.

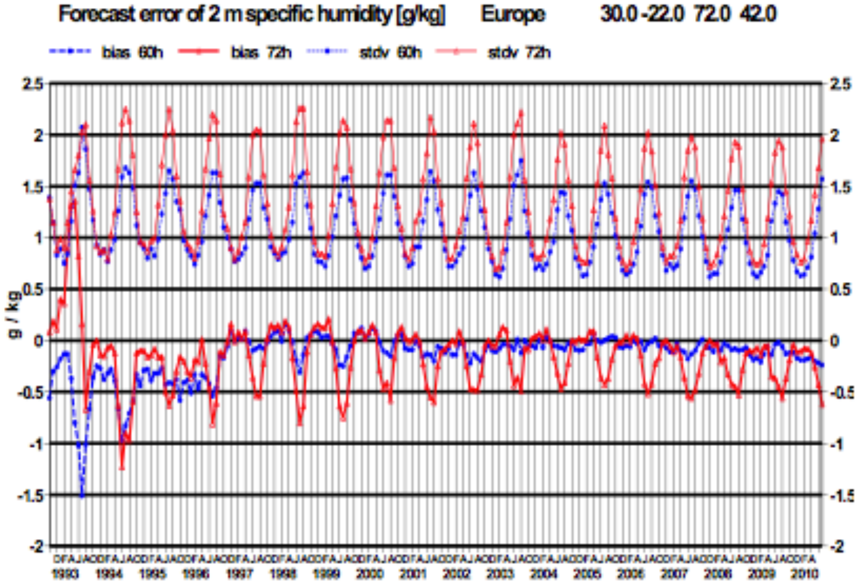

Figure 17: Verification of 2 metre specific humidity forecasts against European SYNOP data on the GTS for 60-hour (night-time) and 72-hour (daytime) forecasts. Lower pair of curves show bias, upper curves are standard deviation of error.

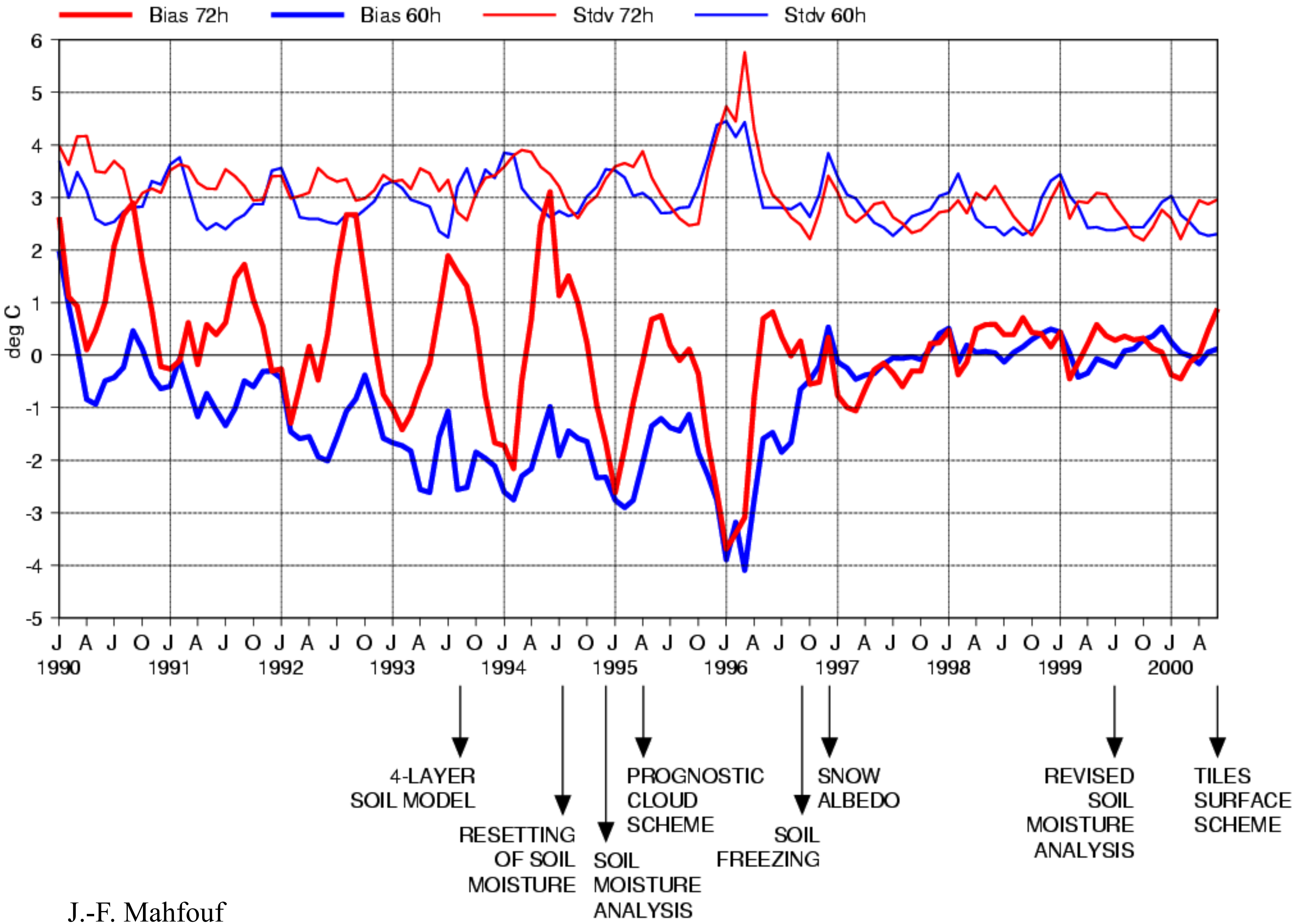
Bias 72h
Bias 60h
Stdv 72h
Stdv 60h
deg C
6
5
4
3
2
1
0
-1
-2
-3
-4
-5
J A J O J A J O J A J O J A J O J A J O J A J O J A J O J A J O J A J O J A J O J A
1990
1991
1992
1993
1994
1995
1996
1997
1998
1999
2000
4-LAYER SOIL MODEL
RESETTING OF SOIL MOISTURE
SOIL MOISTURE ANALYSIS
PROGNOSTIC CLOUD SCHEME
SOIL FREEZING
SNOW ALBEDO
REVISED SOIL MOISTURE ANALYSIS
TILES SURFACE SCHEME

J.-F. Mahfouf

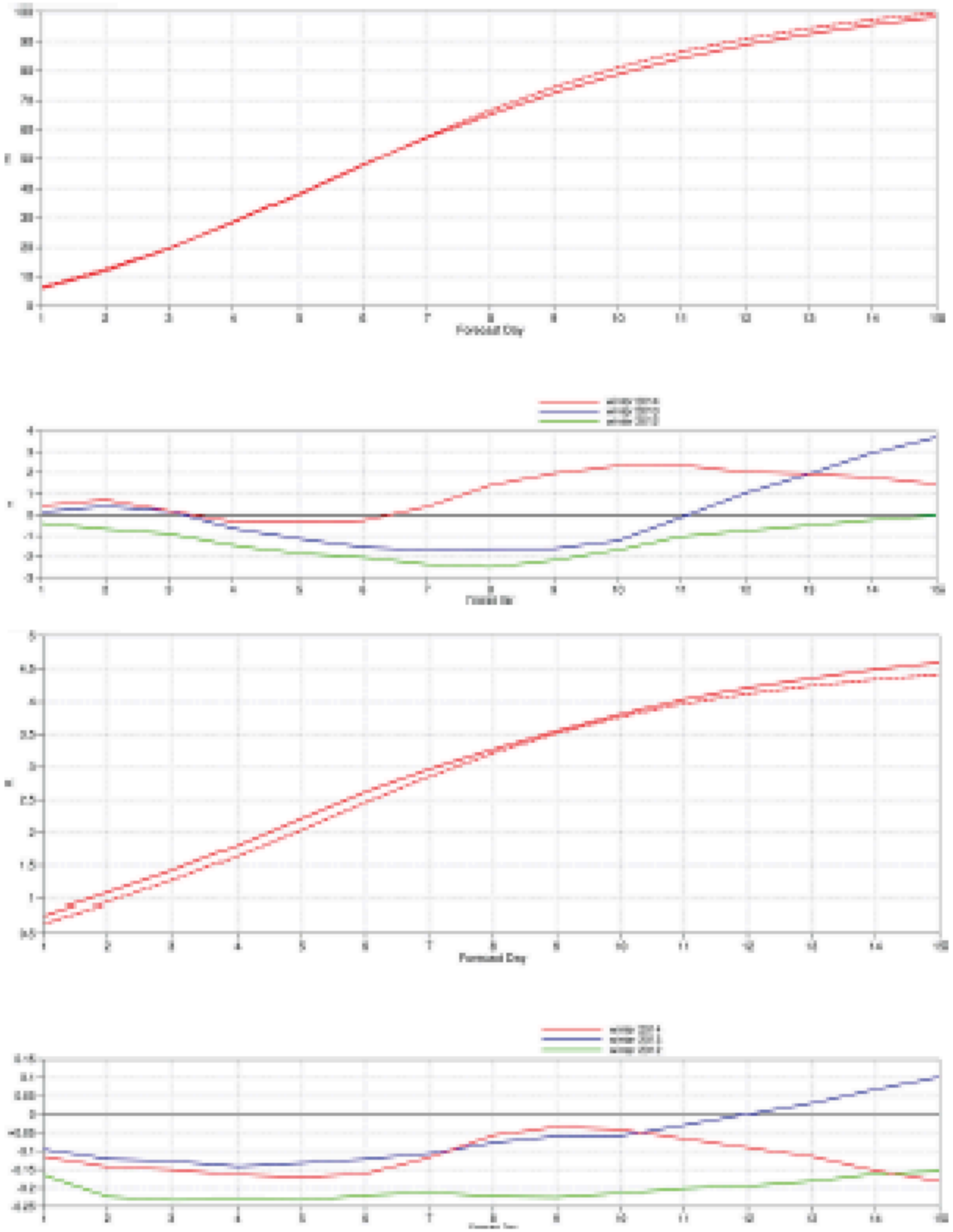

Figure 9: Ensemble spread (standard deviation, dashed lines) and RMS error of ensemble-mean (solid lines) for winter 2013–2014 (upper figure in each panel), and differences of ensemble spread and RMS error of ensemble mean for last three winter seasons (lower figure in each panel, negative values indicate spread is too small); plots are for 500 hPa geopotential (top) and 850 hPa temperature (bottom) over the extratropical northern hemisphere for forecast days 1 to 15.

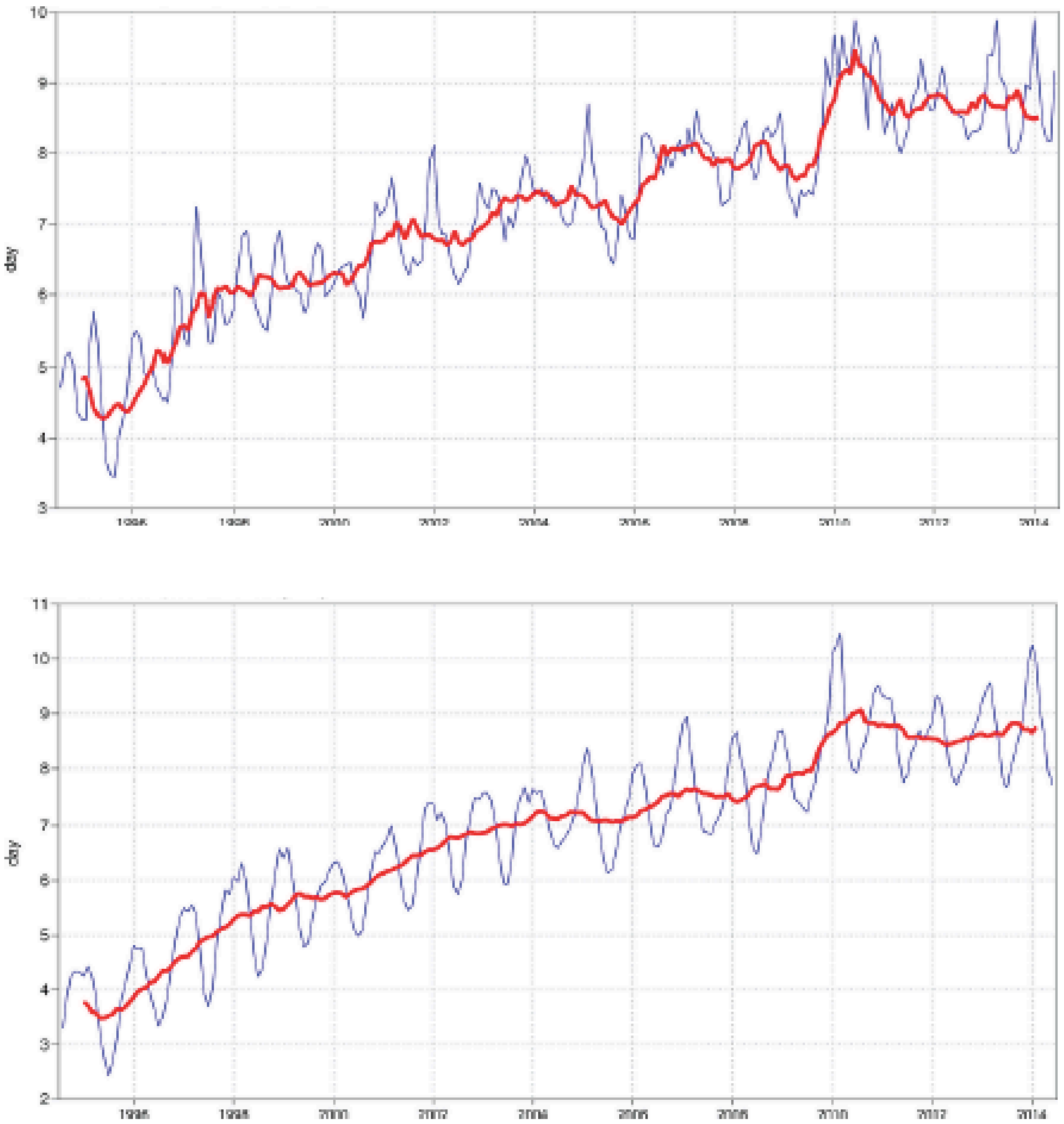

Figure 8: Primary headline score for the ensemble probabilistic forecasts. Evolution with time of 850 hPa temperature ensemble forecast performance – each point on the curves is the forecast range at which the 3-month mean (blue lines) or 12-month mean centred on that month (red line) of the continuous ranked probability skill score (CPRSS) falls below 25% for Europe (top), northern hemisphere extratropics (bottom).

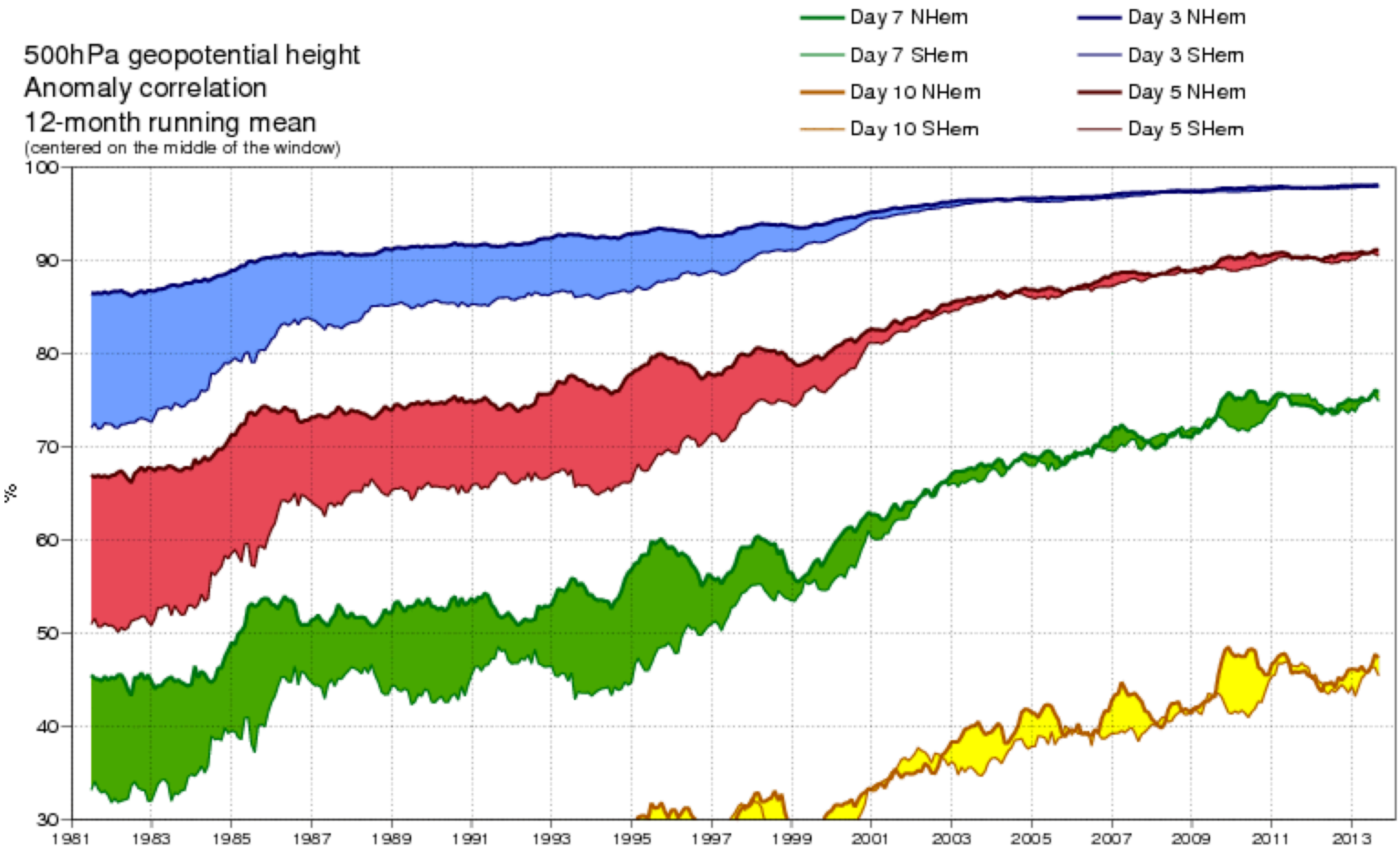

500hPa geopotential height
Anomaly correlation
12-month running mean
(centered on the middle of the window)

Problèmes restants

- Cycle de l'eau (évaporation, condensation, influence sur le rayonnement absorbé ou émis par l'atmosphère)
- Échanges avec l'océan ou la surface continentale (chaleur, eau, quantité de mouvement, …)
- …

ECMWF

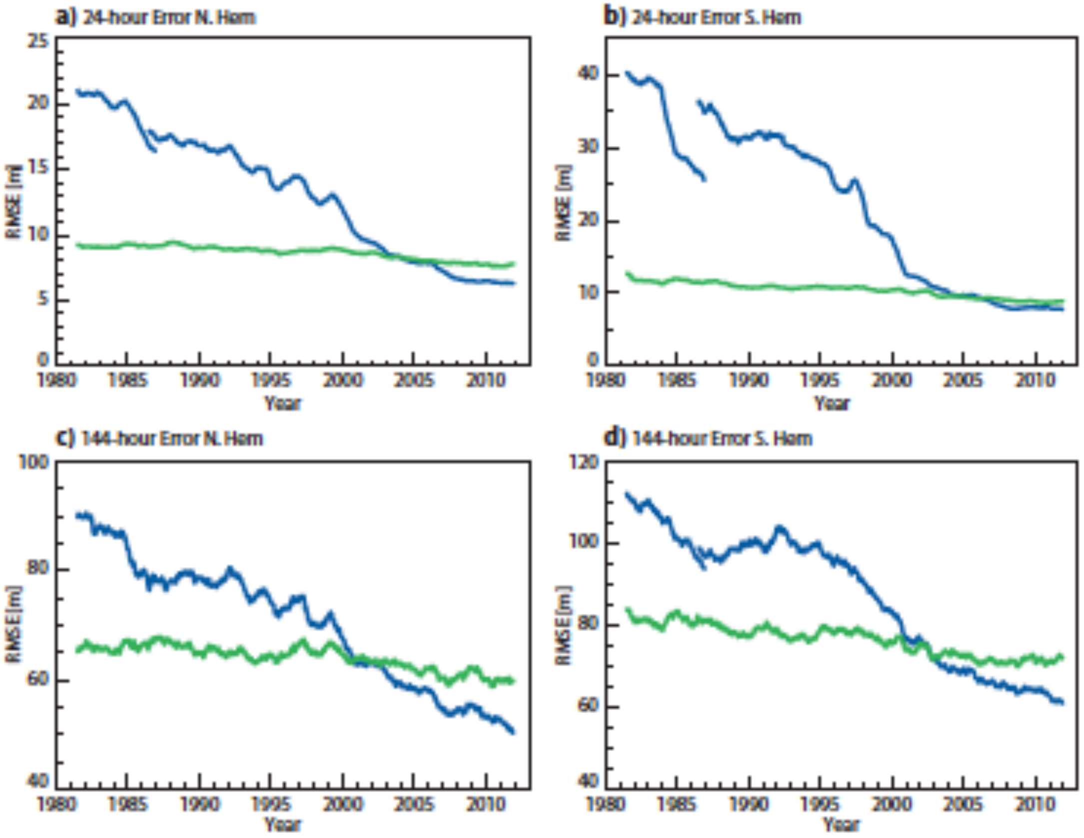

FIG. 3. Evolution of forecast errors from 1981 to 2012 for N.Hem (a and c) and S.Hem (b and d). Operational forecasts (blue) and ERA Interim (green). Note that before 1986 the operational analysis is used to verify the operational forecasts, after 1986 ERA Interim is used for the verification (with an overlap of 6 months present).

Magnusson and Källén, 2013, *Mon. Wea. Rev.*, **141**, 3142–3153

Fig. 1: Members of day 7 forecast of 500 hPa geopotential height for the ensemble originated from 25 January 1993.

Figure 6 Hurricane Katrina mean-sea-level-pressure (MSLP) analysis for 12 UTC of 29 August 2005 and t+84h high-resolution and EPS forecasts started at 00 UTC of 26 August:

1st row: 1^{st} *panel: MSLP analysis for 12 UTC of 29 Aug*
2^{nd} *panel: MSLP t+84h* T_L*511L60 forecast started at 00 UTC of 26 Aug*
3^{rd} *panel: MSLP t+84h EPS-control* T_L*255L40 forecast started at 00 UTC of 26 Aug*
Other rows: 50 EPS-perturbed T_L*255L40 forecast started at 00 UTC of 26 Aug.*

The contour interval is 5 hPa, with shading patters for MSLP values lower than 990 hPa.

ECMWF, Technical Report 499, 2006

Pourquoi les météorologistes ont-ils tant de peine à prédire le temps avec quelque certitude ? Pourquoi les chutes de pluie, les tempêtes elles-mêmes nous semblent-elles arriver au hasard, de sorte que bien des gens trouvent tout naturel de prier pour avoir la pluie ou le beau temps, alors qu'ils jugeraient ridicule de demander une éclipse par une prière ?[...] un dixième de degré en plus ou en moins en un point quelconque, le cyclone éclate ici et non pas là, et il étend ses ravages sur des contrées qu'il aurait épargnées. Si on avait connu ce dixième de degré, on aurait pu le savoir d'avance, mais les observations n'étaient ni assez serrées, ni assez précises, et c'est pour cela que tout semble dû à l'intervention du hasard.

H. Poincaré, *Science et Méthode*, Paris, 1908